Jurnal Tribologi 37 (2023) 14-27

Influence of ceramic particles size on the incorporation of SiC into stainless steel material using 480 J/mm heat input for tribological applications

Lailatul Harina Paijan [1*], Md. Abd. Maleque [2], Bello Kamilu Adeyemi [3], Mohd Fauzi Mamat [1], Nur Izan Syahriah Hussein [4]

[1] Fakulti Teknologi Kejuruteraan Mekanikal & Pembuatan, Universiti Teknikal Malaysia Melaka, Hang Tuah Jaya, 76100 Durian Tunggal, Melaka, MALAYSIA.
[2] Department of Manufacturing and Materials Engineering, Kuliyyah of Engineering, International Islamic University of Malaysia, 53100 Gombak, Kuala Lumpur, MALAYSIA.
[3] Department of Metallurgical and Materials Engineering, Ahmadu Bello University Zaria, NIGERIA.
[4] Fakulti Kejuruteraan Pembuatan, Universiti Teknikal Malaysia Melaka, Hang Tuah Jaya, 76100 Durian Tunggal, Melaka, MALAYSIA.
*Corresponding author: lailatulharina@utem.edu.my

KEYWORDS

SiC ceramic particles
Tribological
Duplex stainless steel
Hardness
Wear

ABSTRACT

The objective of the present study is to deposit highly wear resistant silicon carbide (SiC) ceramic particles on Duplex-2205 using tungsten inert gas (TIG) torch arc cladding at a heat input of 480 J/mm. The influence of various SiC ceramic particles size ranging from 20 µm to 100 µm on microstructure, hardness and linear motion reciprocating wear test was studied. It was found that the hardness properties for 60 µm and 100 µm samples were generally higher than 20 µm and this was believed owing to the presence of the dendrite microstructure. Furthermore, it was found that wear rate and friction coefficient of larger particle size produced better wear resistance. The tribological properties of the clad layer were increased further due to the well dispersion of the dendrites structure in the SiC-DSS layer. The strongest clad layer consisted of 100 µm SiC particle size and had a hardness value of 750 Hv, wear rate of 4.13 mm^3/Nm and friction coefficient of 0.49.

Received 15 April 2022; received in revised form 20 July 2022; accepted 15 September 2022.
To cite this article: Paijan (2023). Influence of ceramic particles size on the incorporation of SiC into stainless steel material using 480 J/mm heat input for tribological applications. Jurnal Tribologi 37, pp.15-28.

1.0 INTRODUCTION

Nowadays, the SiC has been developed into a high-quality technical grade ceramic with very good mechanical properties. It is used in abrasives, refractories, ceramics and numerous high-performance applications. Due to the high hardness, melting point and good chemical stability of SiC, it can be used as coating reinforcement for surface modification to enhance the surface characteristics of material on hardness and wear behavior (Buytoz, 2006; Mridha & Baker, 2007; Lailatul & Maleque 2017). To achieve this purpose, the surface melting process is required by depositing the SiC powder with desirable composition on the surface of materials are simultaneously melted and rapidly solidified using TIG torch or laser techniques to form the composite coating.

The incorporation of hard ceramic materials to produce a composite layer is a popular method because it can tailor the surface to suit the requirements for many applications. Normally, surface modification by the incorporation of hard ceramic materials is applied to increase wear and corrosion resistance and to prolong its service life. This approach is considered a newly developed type of surface modification that involves dispersion of abrasive ceramics particulate into the metal surface.

Surface melting by incorporation of ceramic particles can produce a composite layer that can enhance the surface hardness and tribological behavior of material. In this process, the ceramic particles with desirable composition are homogeneously deposited onto the surface of the substrate material. The commonly used hard carbide particles to produce ceramic composite coatings with this melting process are; tungsten carbide, WC (Rong et al., 2016), titanium carbide, TiC (Saroj et al., 2017) and SiC (Maleque et al., 2018). The heat sources such as laser, electron beams or TIG torch were used to melt the ceramic particles and substrate material to produce the composite coating (Maleque & Adeleke, 2013, Lailatul & Maleque 2018).

Saroj et al., (2017) have found that the TiC reinforced Inconel825 composite coating on AISI 304 steel substrate were successfully developed by melting process in argon environment under a TIG torch with the current of 90A. With the increment of TiC content in the modified surface, the hardness values also increase until 1100 Hv. The wear behavior analysis demonstrated that the TiC-Inconel825 coating provides the improvement with the addition of the TiC content in the coating.

Paraye et al., (2021) investigated the incorporation of in-situ TiC into the carbon steel fabricated by TIG torch arc welding. The microhardness of the surface composite was increased by 150% to the substrate metal. The increment of hardness is due to the combined effect of bainite matrix along with the precipitated TiC particles.

Mridha & Baker (2007) demonstrated that the formation of composite layers was observed on commercial purity titanium surfaces deposited with 3 μm of SiC using laser beam technique. In this investigation, the SiC particles completely dissolved in all the tracks producing a complex and inhomogeneous microstructure of dendrites and needle particles. The surface hardness developed 5.6–15 times higher than the base hardness (150 Hv) depending on the dendrite population. The large surface area for an equivalent volume fraction of the 3 μm SiC particles is considered to have a high laser coupling action and hence absorbed more heat energy to produce deeper melt depth compared to those produced using the 6 μm SiC.

Munoz-Escalona et al., (2016) revealed that the incorporation of SiC into the microalloyed steel surface produced the increment of surface hardness from 200 to 800 Hv which is almost 300 % higher than substrate material. The SiC powder that deposited on top of the steel surface was incorporated into the melt zone during heating and melting using TIG torch process. The width of

the fusion zone was increased by using 75 μm SiC particle size compared to 1 μm SiC particle size. A higher percentage of silicon was observed at the bottom of the fusion zone than at the surface.

Ramprasad (2015) demonstrated that the embedment of SiC in the surface layer using TIG torch melting has significantly increased the tensile strength and hardness of the Al 6061 alloy steel. The increase in tensile strength was a result of the presence of SiC particles in the composite which contributed to the effective dislocation barriers. The SiC particles have contributed to higher strength of the weld joint as compared to the base due to the grain refining effect due to the heat of welding.

Brytan et al., (2011) investigated the SiC powder preplaced on ferritic, austenitic and duplex stainless steel which melted with a laser surface alloying technique. Based on the result, the laser alloyed layers produced on the surface and provide a significant improvement in wear resistance. The highest wear resistance was obtained on duplex stainless steel material.

Most of the previous studies mentioned earlier have shown that surface modifications with WC, TiC or SiC into duplex stainless steel using TIG torch melting are not done yet. Several research works found in the literatures focus on melting using different alloying powders and substrate materials via TIG torch and laser cladding. Therefore, in this study, research is carried out to employ this approach for DSS effectively and efficiently to produce a hard layer on the surface of DSS.

2.0 MATERIALS AND METHODS

2.1 Materials

For the SiC-DSS coating, the SiC was pre-deposited on a DSS steel plate (50 mm x 33 mm x 10 mm). The DSS material was received from Outokumpu, Mitsui, Sumitomo, Tokyo Japan. AISI Duplex-2205 grade is chosen due to this grade is cost and weight savings (pressure vessels) compared to AISI 316L. In addition, the AISI Duplex-2205 grades represent nowadays about 85% of the total duplex production (Charles). The surface of the DSS plate was undergone a milling process to cut away the unwanted material on the surface sample to remove the swarf and processing residues and provide a uniform flat surface of the sample. Then, the sample was ground using silicon emery paper and thoroughly cleaned in acetone and running water.

2.2 SiC Ceramic Powder Pre-Deposited

In this study, the silicon carbide with a particle size of 20 μm, 60 μm and 100 μm (supplied by Innovative Pultrusion Sdn. Bhd.) was used as a reinforcement material to enhance the surface properties of DSS. The reason for using a variation of particles size is based on fine particle size (20 μm), intermediate particle size (60 μm) and coarse particle size (100 μm) in the development of the TIG melted layer DSS as mentioned by Maleque et al., (2016). These variations are required to observe the influence of different particle sizes on the surface characteristics in terms of microstructure, hardness and tribological properties. For surface modification purposes, the ceramic particle was preplaced on the surface material prior to TIG arc cladding. The SiC powder needs to be transformed into paste form by adding two drops of polyvinyl acetate (PVA), one drop of alcohol and distiller water. Then, the paste form was placed on the surface material and heated in the furnace for 1 hour by maintaining a temperature of 80ºC to remove the moisture and ensure the ceramic particles adhered consistently to the substrate surface during TIG arc melting process.

2.3 Development of SiC Coated DSS

TIG arc technique was employed using Telwin-Miller 165 welding machine. The welding electrode used is a tungsten electrode with 2% thorium. The element of thorium is added to the tungsten electrode to create an electrode alloy that can improve arc stability, emissivity and bring higher melting points. The electrode is a rod shape with a length of 150 mm and diameter of 3.2 mm. In order to provide an effective TIG arc, the electrode end must have the shape of a pointed cone (point angle approximately 10°). To meet this purpose, the electrode tip was ground using a silicon carbide wheel to sharpen the electrode end. The TIG torch was attached to a mounting table with a provision to provide controlled linear motion. The single track and multi-track of a clad layer were obtained through the movement of the worktable. A smooth arc was managed by maintaining a 1 mm gap between the electrode and deposited SiC sample using a transverse speed of 1 mm/s. The TIG arc was shielded by supplying the argon gas at the flow rate of 15 L/min. The heat input for this study was carried out at 480 J/mm.

After the development of the clad layer with specified single and multi-track using different SiC particle sizes, the SiC-DSS sample was cleaned up to remove the excessive ceramic particles and then cut the cross-section using a wire cut electrical discharge machine (EDM). Then, the samples have undergone metallography grinding and polishing method for further investigation.

2.4 Microstructural Behavior

From the single track of clad layer, the cross-section of the clad layer was examined under scanning electron microscopy (SEM) using model JEOL JSM 5600 and energy-dispersive X-ray (EDX) spectroscopy using model ISIS. The microstructural behavior of the clad layer was observed in the structural changes after the deposition of SiC into DSS surface. Moreover, the specific region of the structural changes in the clad layer was identified in terms of the presence of the silicon and carbide.

2.5 Vickers Micro Hardness

The hardness values were measured using a Vickers micro-indentation hardness tester (model: Wilson Wolpert) using a pyramid diamond indenter with 500 gf load and 10 second indentation time. The hardness profile of the clad layer cross-section was attained by measuring the micro-hardness value at the center region of a single track from the top surface towards substrate material. Five indentations were conducted for each sample and the average of the measurement was recorded as a result.

2.6 Reciprocating Wear Testing

In order to identify the behavior of wear characteristics of the clad layer obtained from the multi-pass track, the samples were assessed through a linear reciprocating wear test using the ball-on-disc method (model: Ducom TR-281-M8) according to ASTM D6079. The samples were sectioned through an EDM wire cut machine to the desired rectangular shape of 15 mm × 15 mm × 6 mm. The sharp edges and unwanted impurities present on the surface clad layer were refined with 400 and 800-grade polishing paper to ensure smooth contact between the SiC-DSS coated layer and counterpart material of alumina ceramic ball. The schematic representation of the linear motion of an alumina ceramic ball on the SiC-DSS clad layer is shown in Figure 1, and the test conditions are shown in Table 1. The wear rate value was measured in terms of weight loss of the SiC-DSS clad layer using weight balance. Meanwhile, the coefficient of friction was recorded directly through the Winducom Software from the wear tester machine. Each measurement is

taken three times for each sample. The wear rate of the sample is calculated using the following standard formula and expressed as mm^3/Nm, as shown in equation 1. Furthermore, the pattern of the worn surface morphology after the linear motion reciprocating test is examined under SEM.

$$\text{Wear rate} = \frac{\text{Weight loss } (g) \Big/ \text{Density } (g/mm^3)}{\text{Normal load } (N) \times \text{Reciprocating distance } (m)} \quad (1)$$

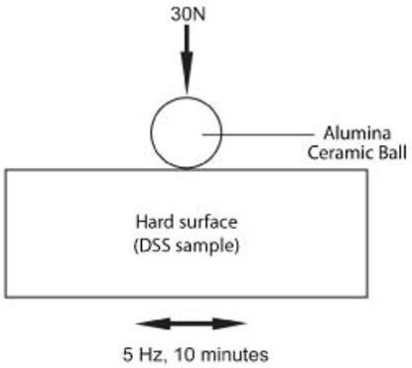

Figure 1: Schematic representation of the linear motion of alumina ceramic ball on the SiC-DSS clad layer.

Table 1: Wear test condition.

Specimen	**Liner motion reciprocating wear test condition**
Applied load	30 N
Frequency	5 Hz
Wear test duration	10 minutes
Counter-part body	6 mm diameter Alumina ceramic ball

3.0 RESULTS AND DISCUSSION

3.1 SEM Image of Surface Coated DSS

Figure 2(a-c) show the SiC ceramic particles with different particle size of 20 µm, 60 µm and 100 µm before the TIG welding process. The microstructure is observed under SEM machine with a magnification of X270. The SiC ceramic particles formed in various shapes consist of cubic and hexagonal structures.

The cross-sectional view of the melt pool for TIG torch melted processed with different SiC particle sizes showed a hemispherical shape as shown in Figures 3(a-c). The Gaussian energy distribution of the torch which has been known to have high energy intensity in the middle region and gradually decrease to the edges is responsible for producing such a hemispherical melt shape and a similar observation was found by Mridha et al., (2012). With 20 µm of SiC particles size in a sample using 20µm SiC particle size, the melt depth value is 1.01 mm. This value is lower than the sample obtained from 60 µm SiC particle size with a melt depth value of 1.42 mm when processed

under the same heat input of 480 J/mm. It can be attributed to the fact that the molten pool of smaller SiC particle size solidified faster than larger SiC particle sizes, thus producing the lowest melt pool depth. This suggests that smaller particle sizes produce less viscous melt compared to larger particle sizes. Therefore, the melt pool can solidify faster than the viscous melt pool.

The highest melt depth was obtained from 100 µm SiC particle size with a value of 1.91 mm. The presence of a larger SiC particle size is responsible for the high absorption of heat input to produce deeper melt depth compared to those produced using a smaller particle sizes. Similar observation has been reported by Munoz-Escalona et al. (2016) in which a wider cross-sectional area and a slight increase in depth were obtained for larger particles of SiC in micro-alloyed steel.

Figures 4(a-c) demonstrate the SEM image of the single track SiC-DSS coating layer deposited with 20 µm, 60 µm and 100 µm SiC particle size. All figures were labeled with regions A, B and C for EDX spectra result that explained in the next section. Based on the SEM image of an etched sample, it was revealed that the clad layer of the TIG arc was successfully developed with the incorporation of SiC ceramic particles uniformly dispersed on DSS via the TIG torch melting process which promotes the formation of dendrite microstructure. Similar findings have been observed in other studies by Singh et al. (2020) found that the dendritic structures were observed when the WC was added as reinforcement on AISI 304 steel manufactured by TIG torch cladding. Moreover, the population of dendrites microstructure varies owing to the different sizes of the ceramic particles. The image indicated that the population of the 20 SiC particles size experienced a lesser dendrite population compared to 60 µm and 100 µm. It also can be observed that the dendrite shape is a fine and thin structure with a mixture of partial and unmelted dissolved SiC in the clad layer of 20 µm, as can be seen in Figure 4a.

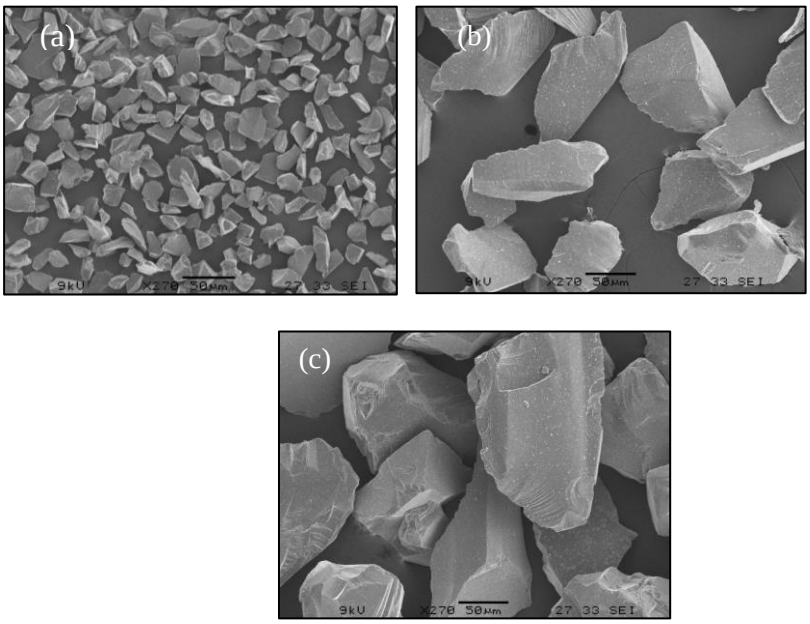

Figure 2: SEM micrograph of SiC ceramic particles with different particle size at magnification of X270; (a) 20 µm, (b) 60 µm and (c) 100 µm.

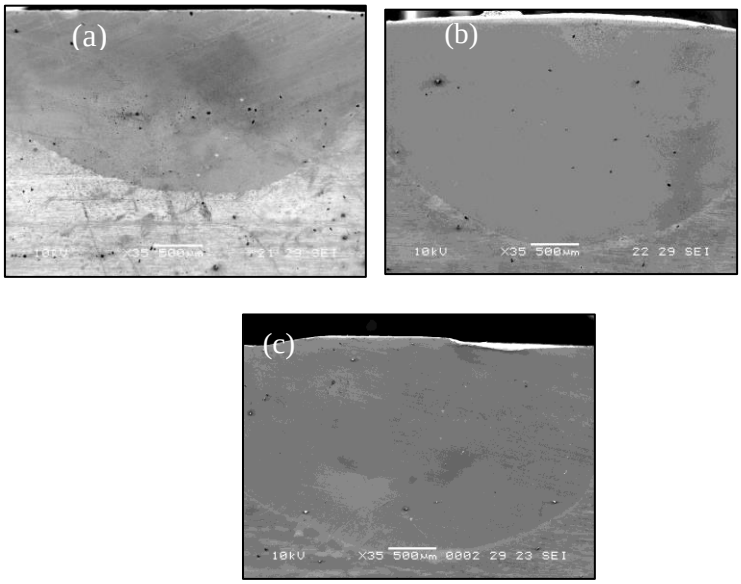

Figure 3: Cross sectional view of melt pool geometry of TIG torch melted DSS using (a) 20 µm, (b) 60 µm and (c) 100 µm.

As compared to 60 µm particle size, the clad layer exhibited a higher SiC population and distributed homogeneously in the matrix of DSS as can be seen in Figure 4b. Moreover, the larger particle size of 100 µm exhibited a more compact SiC population and dissolved uniformly contains partial and complete dissolved SiC as can be seen in Figure 4c. This phenomenon is contributed by larger particle size resulting in more ceramic particles melting and dissolved in the DSS matrix and the results are confirmed in EDX result analysis.

Figures 5(a-c) give the percentage of the SiC to confirm the presence of ceramic particles in the SiC-DSS clad layer. According to the EDX results, it could be initially confirmed that the existence of reinforcing particles was SiC. In Figure 5a, the EDX results (region A in Figure 4a) demonstrated a low percentage of silicon (Si) with 7.94% and carbon (C) of 7.60 % due to the lower particle size of 20 µm in the clad layer. Meanwhile, in Figure 5b it can be seen that the composition of the ceramic particles reduced for 60 µm with the Si value of 4.56 % but increased for carbon value by 7.93 %. On the other hand, the SiC population continuously increased in the clad layer under TIG arc melting using a particle size of 100 µm with a value of 7.82 % for Si and 9.93 % for carbon, as presented in Figure 5c.

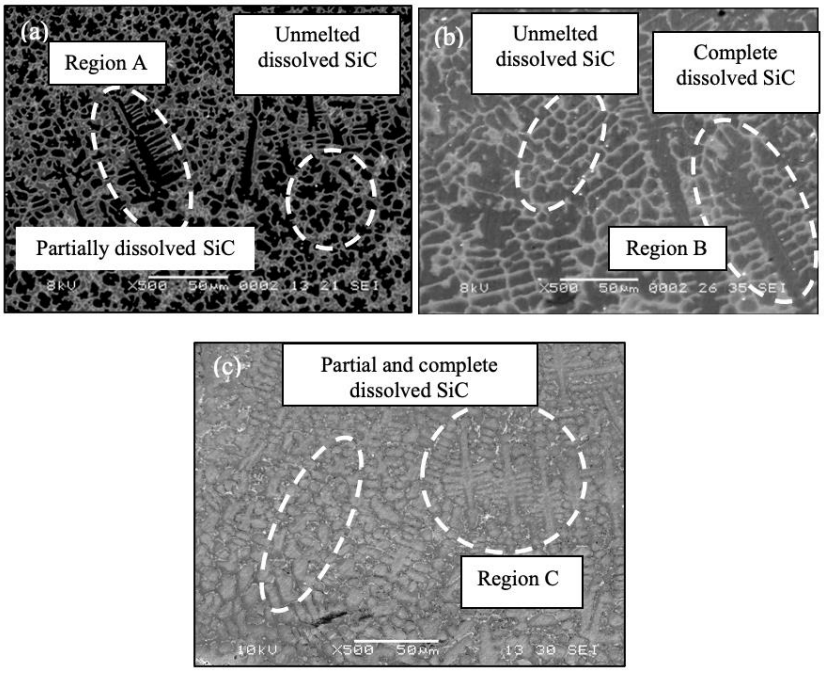

Figure 4: SEM images for surface SiC-DSS under TIG arc heat input at 480 J/mm using SiC particle size of (a) 20 µm (b) 60 µm and (c) 100 µm.

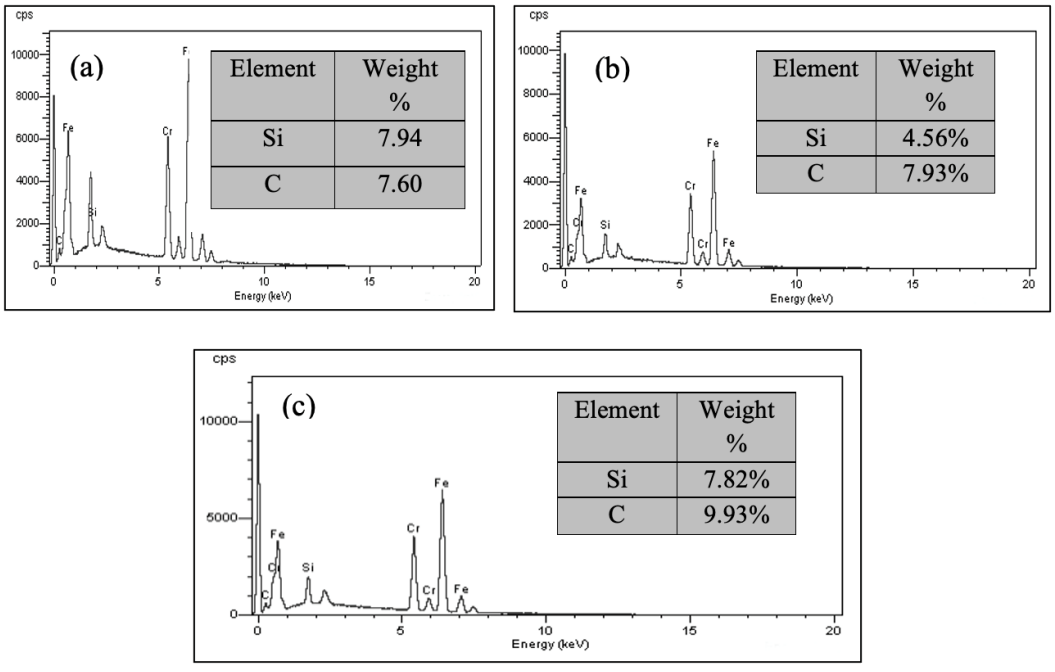

Figure 5: EDX spectra within dendrite correspond to (a) region A in Figure 2(a), (b) region B in Figure 2(b) and (c) region C in Figure 2(c).

3.2 Vickers Micro Hardness Profile of Surface Coated DSS

To figure out the discrepancy in the micro-hardness value at different positions of the SiC-DSS clad layer, the micro-hardness value was measured along the centerline of the single track. The mean hardness values assessed from a different region were plotted considering the distance from the top surface, as depicted in Figure 6. For almost all particle sizes, the high hardness values were recorded at the clad layer, which is dropped slowly from the top surface towards the substrate. However, a substantial discrepancy in the hardness value can also be observed for different SiC particle sizes ranging from 20 µm to 100 µm. Furthermore, relatively lowest hardness value was attained in the clad layer with 20 µm particle size with a hardness value of 650 Hv, and for increasing the particle size (60 µm and 100 µm), the hardness value measured in the centerline of the tracks obviously increased. Corresponding to the hardness values with SEM cross-sectional images of the clad layer revealed that for lower SiC particle size, the population of the SiC particles in the clad layer is reasonably low, which resulted in a lower micro-hardness value. Accordingly, the hardness top surface was continuously increased by using a higher particle size of 60 µm and 100 µm with a high hardness value of 701.9 Hv and 750 Hv, respectively. The results obtained agreed with previous work carried out by Munoz-Escalona et al. (2016) whereby the 75 µm SiC particle size produced higher hardness compared to 1 µm SiC particle size via the TIG torch cladding process. As evident from the microstructural analysis, both samples exhibited a higher population of SiC particles with the increment of SiC detection as shown in EDX results.

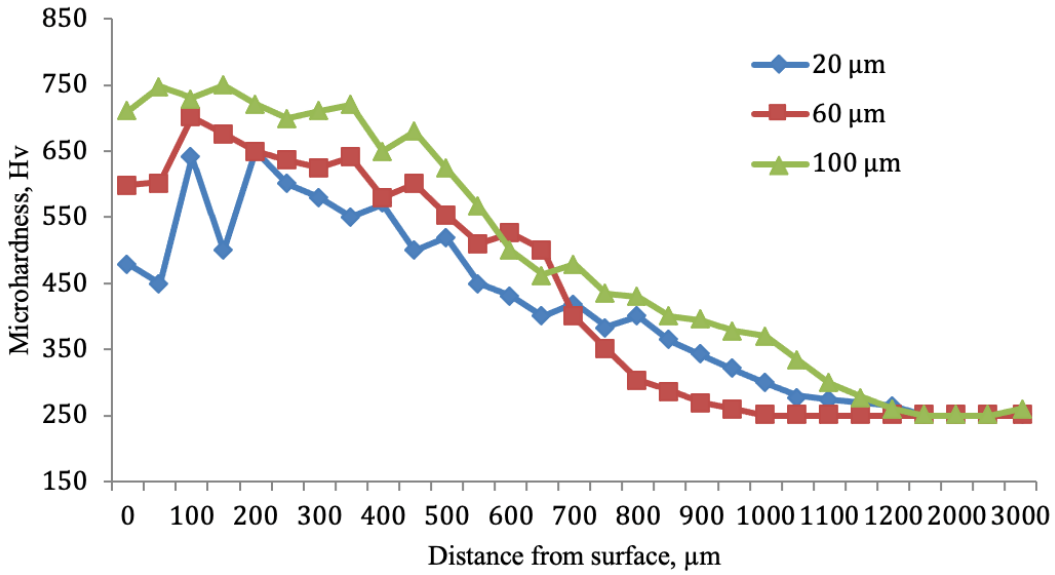

Figure 6: Micro-hardness variation along the centerline towards substrate material of the TIG cladding SiC–DSS layer for 20 µm, 60 µm and 100 µm under heat input of 480 J/mm.

3.3 Linear Motion of Reciprocating Wear

The tribological behavior of the SiC-DSS clad layer produced under various SiC ceramic particle size was assessed through a linear motion reciprocating test carried out under an alumina ceramic ball. Figure 7 demonstrates the wear rate of different particle sizes of 20 µm, 60 µm and 100 µm under heat input of 480 J/mm. It was found that the wear rate for 20 µm SiC particle size is 4.26 x 10^{-4} mm^3/ Nm. Meanwhile, for 60 µm SiC particle size, the wear rate obtained in this sample is 4.15 x 10^{-4} mm^3/ Nm. On the other hand, 100 µm SiC particle size attained the lowest wear rate with 4.13 x 10^{-4} mm^3/ Nm. Generally, the wear rate increases with an increased in SiC particle size, dendrite population in the clad layer and the trend matches the hardness results. This is believed to occur due to larger particle size producing a dense and well dispersion of dendrite concentration in the clad layer and therefore increased hardness values as mentioned earlier. It can be concluded that there is a direct correlation between wear rate and hardness performance of the SiC-DSS clad layer.

The variations of the friction coefficients of the SiC-DSS clad layer are depicted in Figure 8. The Friction coefficients of the clad layer for 20 µm, 60 µm and 100 µm SiC particle size at a heat input of 480 J/mm are 0.60, 0.57 and 0.49, respectively. It can be seen that the friction values of the clad layer consistently reduced with the increment of particle size of SiC. The results suggest that the highest value for friction using 20 µm might be obtained by the lower hardness of this sample. In contrast to the usage of the 60 µm and 100 µm SiC particle size, the hardness value was higher, and a high concentration of dendrite formation compared to the 20 µm sample leads to the reduction of the friction coefficient value. It can be revealed that the tribological properties of the SiC-DSS clad layer could improve the wear rate and friction coefficient of the clad layer. It can be seen that the improvement of wear test by deposition of ceramic particles on steel surface has occurred similarly to that obtained in previous research by Prasad et al. (2020).

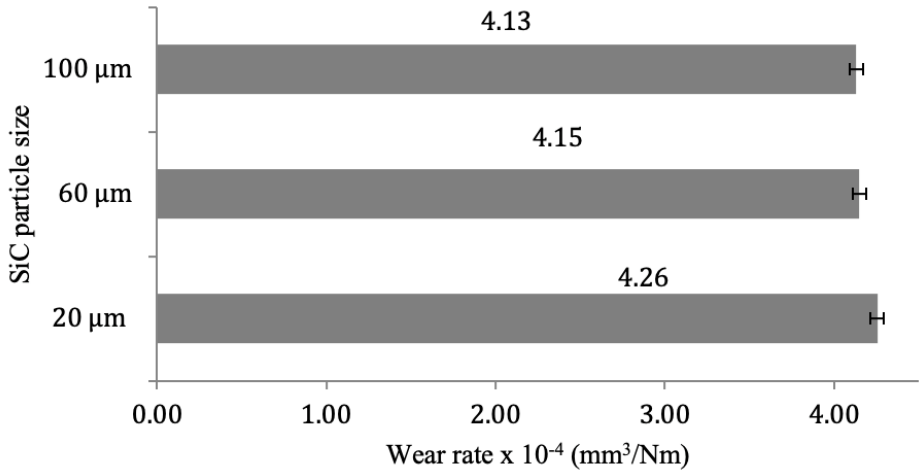

Figure 7: Wear rate of the SiC-DSS clad layer attained for different SiC particle size.

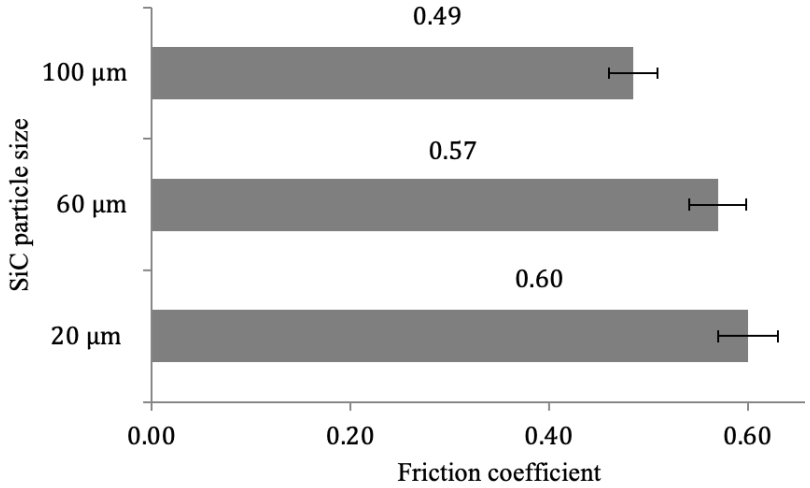

Figure 8: Friction coefficient of the SiC-DSS clad layer attained for different SiC particle size.

3.4 Worn Surface Analysis

The wear behavior of the SiC-DSS clad surfaces were evaluated from the SEM images taken at X250 magnifications after the reciprocating wear test as presented in Figure 9. The images demonstrate the formation of wear tracks over the surface of the clad layer. It can be seen from Figures 9 (a-c), whereby the worn surface became clean and smooth from moderate striations for 20 µm SiC particles size into mild striations for 60 µm and 100 µm SiC particles. The improvement in wear track for reciprocating wear can be attributed to the deposition of the SiC into DSS clad layer with larger particle size leading to the homogeneous distribution and compact population of dendrite formation.

It also showed that SiC-DSS clad layers with a larger particle size of 100 µm SiC were able to resist and withstand the load with very mild striation. During a wear test, the dendrites not only strengthened the structure but also prevented rubbing from plastic flow, which limited the scarring of the TIG melted sample at high reciprocating speed (Peng, 2012). Moreover, the increased of the metallurgical bonding strength and strong mechanical interlocking between the SiC particle and the DSS matrix helped to prevent severe wear. The hard phase of the SiC particles contributed to the excellent wear resistance of the SiC-DSS clad layer.

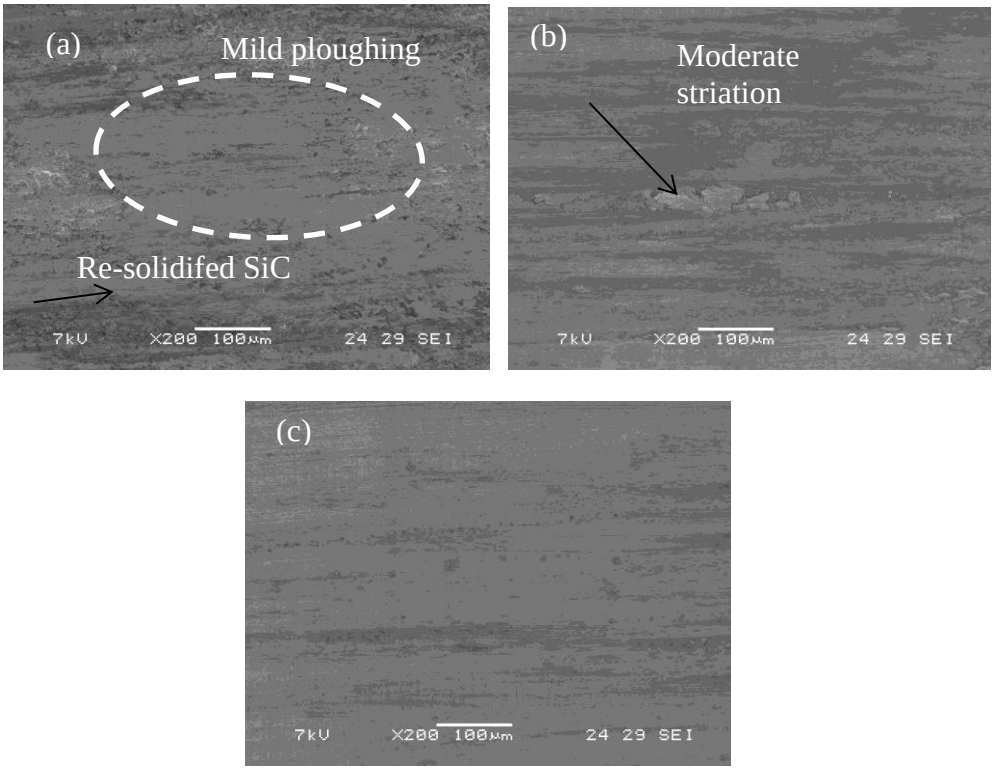

Figure 9: SEM image of the SiC-DSS clad layer attained for different SiC particle size; (a) 20 µm, (b) 60 µm and (c) 100 µm.

CONCLUSIONS

The application of SiC ceramic particles deposited into the DSS surface using the TIG torch process for surface modification is now well established. The present investigation has shown several conclusions as follows;

(a) The influence of the different SiC particle sizes can increase the hardness of the DSS top surface clad layer by about 650 ~ 750 Hv with the increase of SiC particle size from 20 µm to 100 µm.
(b) It was found that SiC particle size had the greatest influence on hardness value followed by wear rate and friction coeficient.
(c) The improvement of the hardness and tribological properties was correlated well with the dendrite microstructure containing dissolution of SiC particle in the DSS matrix.
(d) The 100 µm SiC particle size provides the most significant influence on the improvement of the tribological properties.

ACKNOWLEDGMENTS

The financial support for this research was provided by Short Term Grant UTeM 2022 (S01895-PJP/2022/FTKMP) and Ministry of Higher Education Malaysia for Fundamental Research Grant Scheme (FRGS) with Project Code: FRGS/1/2015/TK05/UIAM/01/1. Authors also are grateful to the International Islamic University Malaysia and Universiti Teknikal Malaysia Melaka for the support that made this study possible.

REFERENCES

Brytan, Z., Dobrzański, L. A., & Pakieła, W. (2011). Laser surface alloying of sintered stainless steels with SiC powder. Journal of Achievements in Materials and Manufacturing Engineering, 47, 42–56.

Buytoz, S. (2006). Microstructural properties of SiC based hardfacing on low alloy steel. Surface & Coating Technology, 200, 3734-3742.

Charles, J. Past, Present and Future of the duplex stainless steels. France.

Lailatul, P. H. and Maleque, M. A. (2017). Surface Modification of Duplex Stainless Steel with SiC Preplacement Using TIG Torch Cladding. Procedia Engineering, 184, 737 – 742.

Lailatul, P. H. and Maleque, M. A. (2018). Tribological properties of surface coated duplex stainless steel containing SiC ceramic particles. Jurnal Tribologi, 18, 136 – 148.

Maleque, M. A., Radhi, M., & Rahman, M. (2016). Wear study of Mg-SiCp reinforcement aluminium metal matrix composite. Journal of Mechanical Engineering and Sciences, 10, 1758–1764.

Maleque, M.A. and Adeleke, S.A. (2013). Surface Alloying of CP-Ti Using preplaced Fe-C-Si powder by Tungsten Inert Gas Torch Technique. In International Conference on Mechanical, Industrial and Materials Engineering, 668 - 673.

Maleque, M.A., Lailatul, H., Bello, K. Azwan, M. and Rahman, M. M. (2018). Tribological properties of surface modified Ti-6Al-4V alloy under lubricated condition using Taguchi approach. Jurnal Tribologi, 17, 15-28.

Mridha, S., & Baker, T. N. (2007). Incorporation of 30 μm SiCp into Titanium surfaces using a 2.8 kW laser beam of 186 and 373 MJ/m^2 energy densities in a nitrogen environment. Journal of Materials Processing Technology, 185(1–3), 38–45.

Mridha, S., Idriss, A. N. M., & Baker, T. N. (2012). Incorporation of TiC particulates on AISI 4340 low alloy steel surfaces via tungsten inert gas arc melting. Advanced Materials Research, 445, 655–660.

Munoz-Escalona, P., Mridha, S., & Baker, T. N. (2016). Effect of silicon carbide particle size on microstructure and properties of a coating layer on steel produced by TIG technique. Advances in Materials and Processing Technologies, 1–11.

Paraye, N.K., Ghosh, P.K. and Das, S. (2021). Surface modification via in situ formation of titanium carbide in ferrous matrix through TIG arcing. Material Letters, 283, 128723.

Peng, D. X. (2012). Optimization of welding parameters on wear performance of cladded layer with TiC ceramic via a Taguchi approach. Tribology Transactions, 55, 122–129.

Prasad, R., Waghmare, D. T., Kumar, K. and Masanta, M. (2020). Effect of overlapping condition on large area NiTi layer deposited on Ti-6Al-4V alloy by TIG cladding technique. Surface & Coatings Technology, 385, 125417.

Ramprasad, A. (2015). Influence of SiC particles on microstructural characteristics of TIG weld joints of Al 6061-20%SiCp. International Journal of Innovative Science, Engineering & Technology, 2, 132–137.

Rong, T., Gu, D., Shi, Q., Cao, S., & Xia, M. (2016). Effects of tailored gradient interface on wear properties of WC/Inconel 718 composites using selective laser melting. Surface and Coatings Technology, 307, 418–427.

Saroj, S., Sahoo, C. K., Tijo, D., Kumar, K. and Masanta, M. (2017). Sliding abrasive wear characteristic of TIG cladded TiC reinforced Inconel825 composite coating. International Journal of Refractory Metals and Hard Materials, 69, 119–130.

Singh, J., Thakur, L. and Angra, S. (2020). Abrasive wear behavior of WC-10C0-4Cr cladding deposited by TIG welding process. International Journal of Refractory Metals & Hard Materials, 88, 105198.